Spinghar University- Kabul

Spinghar Journal of Biomedical Sciences (SJBS)

Vol. 2, No. 2, Oct 2026, pp.199-225

Homology Modeling, Structural Validation, Active Site Identification, and Binding Pocket Analysis of *Leishmania major* Spermidine Synthase, An in Silico Structural Characterization Study

*Ajazulhaq Haqmal[1,2], Zardar Khan[1], Shamsurrahman Shams[3], Neak Mohammad Momand[3], Sayeed Kashif Sayeedi[3], Mohammad Aslam Bik Danishmal [2], Sher Azam Khan Awrangzai [4], Marwan Ahmad [5]

1. *Department of Chemistry, Faculty of Science, Nangarhar University, Nangarhar, Afghanistan.*
2. *Department of Basic Science, Faculty of Medicine, Spinghar University, Kabul, Afghanistan.*
3. *Department of Clinic, Faculty of Medicine, Spinghar University, Kabul, Afghanistan*
4. *Department of Para Clinic, Faculty of Bio Medical Technology, Spinghar University, Kabul, Afghanistan*
5. *Faculty of Medicine, Spinghar University, Kabul, Afghanistan*

ARTICLE INFO

Type: Original Article
Received: 03/07/2026
Accepted: 25/09/2026

*Corresponding Author:
Ajazulhaq Haqmal

E-mail address:
ajazulhaqhaqmal@gmail.com

DOI:
https://doi.org/10.64444/sjbs.60

ABSTRACT

Background: Leishmaniasis remains a major global health challenge due to limited therapeutic options and emerging drug resistance. *Leishmania major* spermidine synthase (SPDS) is an essential enzyme in polyamine biosynthesis, serving as a critical precursor for the trypanothione antioxidant system. Despite its importance for parasite viability and its absence in human hosts, the three-dimensional architecture of *L. major* SPDS remains experimentally unresolved. Structural characterization is therefore imperative to facilitate the rational design of selective inhibitors targeting this vital metabolic pathway.

Methods: The tertiary structure was predicted via homology modeling using the SWISS-MODEL server and validated through ERRAT, PROCHECK, and Verify3D analysis. Conserved domains were identified using NCBI CD-Search. Binding pockets were characterized via PrankWeb and DoGSiteScorer while potential active site residues were determined through structural comparison with ligand-associated homologous templates and UniProt-annotated catalytic information.

Results: The generated model, based on a *Trypanosoma cruzi* template (67.92% identity), demonstrated high reliability with a GMQE score of 0.87 and an ERRAT factor of 91.034%. Ramachandran plot analysis showed 99.0% of residues in acceptable regions. Pocket 1 was identified as the primary druggable site, exhibiting a volume of 931.34 Å³ and a drug score of 0.83. Eleven conserved binding pocket-associated residues and the UniProt-annotated catalytic residue Asp173 were identified within the active region.

Conclusion: This study establishes a high-quality structural framework for *L. major* spermidine synthase. The identified binding pockets and conserved active-site residues provide essential molecular insights for future virtual screening and structure-based drug discovery efforts aimed at developing potent and selective anti-leishmanial therapeutics.

Keywords: *Leishmania major;* Spermidine synthase; Homology modeling; Structural validation; Active site identification; Binding pocket analysis

Copyright © 2026. Spinghar Journal of Biomedical Sciences, and Spinghar University-Kabul. All rights reserved.
This work is licensed under a Creative Commons Attribution-Noncommercial 4.0 International License

Introduction

Leishmaniasis is one of the most important neglected tropical diseases (NTDs) and remains a major public health concern in many tropical and subtropical regions of the world [1, 2]. The disease is caused by protozoan parasites of the genus *Leishmania* and is transmitted through the bite of infected female phlebotomine sandflies [2, 3]. According to the WHO, leishmaniasis affects millions of people worldwide, with hundreds of millions living at risk of infection [3, 4].

The disease manifests in three principal clinical forms, namely cutaneous, mucocutaneous, and visceral leishmaniasis, each differing in severity and clinical outcome [1, 5]. Among the causative species, *L. major* is one of the primary etiological agents of cutaneous leishmaniasis, producing chronic ulcerative skin lesions that frequently result in permanent scarring, social stigma, and reduced quality of life [5, 6]. Despite continuous efforts toward disease control, the global burden of leishmaniasis remains substantial because of limited therapeutic options, emerging drug resistance, treatment-associated toxicity, and the absence of an effective human vaccine [7, 8].

The survival, proliferation, and infectivity of *Leishmania* parasites depend on a variety of essential metabolic pathways that regulate cellular growth and adaptation to hostile intracellular environments [9]. Among these pathways, polyamine biosynthesis plays a fundamental role in maintaining parasite viability through the regulation of DNA replication, RNA transcription, protein synthesis, oxidative stress responses, and cellular differentiation [9, 10]. Polyamines, including putrescine, spermidine, and spermine, are indispensable for parasite development, making enzymes involved in their biosynthetic pathway attractive molecular targets for rational drug discovery [10,11]. The target protein investigated in the present study is *L. major* spermidine synthase (SPDS; EC 2.5.1.16), encoded by the *LMJF_04_0580* gene and annotated in the UniProt Knowledgebase under accession number Q95Z84 (entry name: Q95Z84_LEIMA). SPDS is a key aminopropyltransferase enzyme that catalyzes the transfer of an aminopropyl group from decarboxylated S-adenosylmethionine (dcSAM) to putrescine, thereby producing spermidine [11, 12]. This enzymatic reaction represents a crucial step in polyamine metabolism and contributes directly to parasite growth, differentiation, and intracellular survival [12, 13]. Furthermore, spermidine serves as a precursor for trypanothione biosynthesis, a unique thiol-containing metabolite that contributes to the protection of trypanosomatid parasites against oxidative stress generated by the host immune system [13, 14].

Although the trypanothione-dependent redox system is a distinctive feature of trypanosomatid parasites and is absent in humans, SPDS itself is also present in the human host and performs an essential function in human polyamine metabolism [14, 15]. Therefore, the absence of the trypanothione pathway in humans alone cannot establish SPDS as a parasite-selective therapeutic target. Instead, the potential selectivity of SPDS-targeted intervention depends on exploitable structural and functional differences between the parasite and human enzymes, particularly within substrate-binding and active-site regions that may permit preferential inhibitor binding [14, 15]. Structural differences between *Leishmania* and human SPDS can be exploited in structure-based inhibitor design, including the identification of compounds predicted to preferentially interact with the parasite enzyme while showing limited interaction with the human counterpart [15]. Accordingly, detailed characterization of parasite SPDS structure, particularly its binding-pocket architecture and active-site residues, is important for evaluating its potential as a selective therapeutic target. Advances in structural biology have signif-

icantly accelerated structure-based drug discovery by providing detailed insights into protein architecture, catalytic mechanisms, ligand-binding regions, and molecular interactions [16]. However, experimentally determined three-dimensional structures obtained through X-ray crystallography, nuclear magnetic resonance spectroscopy, or cryo-electron microscopy remain unavailable for numerous proteins from pathogenic organisms, including several proteins of *L. major* [16, 17]. In such cases, computational structural biology has become an indispensable alternative for predicting protein structures and characterizing their functional properties [17, 18].

Homology modeling is one of the most widely applied computational approaches for predicting the tertiary structure of proteins based on experimentally resolved homologous templates [18, 19]. When sufficient sequence similarity exists between a target protein and a known template, homology modeling can generate reliable structural models suitable for downstream analyses, including structural validation, active-site characterization, ligand-binding pocket prediction, virtual screening, and molecular docking [19, 20]. Nevertheless, the reliability of computational models depends on rigorous quality assessment using complementary validation methods such as Ramachandran plot analysis, ERRAT, Verify3D, QMEAN, GMQE, and structural superposition with experimentally determined template structures [20, 21]. Identification of ligand-binding pockets and catalytically important residues constitutes another essential component of structure-based drug discovery [22]. Although previous studies have highlighted the biological importance of spermidine synthase in polyamine metabolism and have explored its enzymatic function, inhibitory potential, and therapeutic relevance in different trypanosomatid parasites, comprehensive structural information regarding *L. major* spermidine synthase remains limited [22, 23]. Structural investigations have been reported for spermidine synthase enzymes from other trypanosomatid species, including *Trypanosoma cruzi* and *L. donovani*; however, a detailed and systematic structural characterization of *L. major* spermidine synthase has not yet been comprehensively established [23, 24]. Although currently available computational prediction approaches, including AlphaFold-based structural models, have significantly expanded protein structure availability, they generally require additional analyses to evaluate structural reliability, conformational stability, conserved functional regions, catalytic residues, and ligand-binding characteristics [25, 26]. In particular, detailed assessment of binding pockets and active-site architecture, which are essential for structure-based drug discovery, remains insufficiently explored for *L. major* spermidine synthase [26]. Therefore, a comprehensive computational investigation integrating homology modeling, multiple structural validation approaches, structural comparison with experimentally resolved homologous templates, binding-pocket prediction, and active-site identification is required to establish a reliable structural framework for *L. major* spermidine synthase [18, 26].

Such an integrated approach can provide essential molecular insights into the structural organization and functional properties of this enzyme and support future structure-based drug discovery strategies, including molecular docking, virtual screening, and rational design of novel anti-leishmanial therapeutic agents.

The generated structural model and functional analyses provide valuable molecular insights into the architecture of this essential enzyme and establish a structural framework for future molecular docking, virtual screening, and rational anti-leishmanial drug discovery studies. Furthermore, spermidine serves as a precursor for trypanothione biosynthesis, a unique thiol-containing metabolite that protects trypanosomatid parasites against oxidative stress generated by the host immune system [13, 14]. Alt-

hough the trypanothione-dependent redox system is a distinctive feature of trypanosomatid parasites and is absent from humans, SPDS itself is also present in humans and performs an essential function in human polyamine metabolism [14, 15]. Therefore, the absence of the trypanothione pathway alone does not establish SPDS as a parasite-selective therapeutic target. Rather, the therapeutic potential of SPDS depends on the identification and exploitation of structural and functional differences between parasite and human SPDS enzymes, particularly differences within substrate-binding and active-site regions that may permit selective inhibitor binding [14, 15]. Such parasite–host differences in spermidine synthase can be exploited to identify compounds with preferential binding to the parasite enzyme while minimizing interactions with the human counterpart [15]. Accordingly, detailed characterization of the parasite SPDS structure, including its binding-pocket architecture and active-site residues, is an important prerequisite for assessing its potential as a selective drug target.

Therefore, we aimed to perform an integrated *in silico* structural characterization of *L. major* spermidine synthase through homology modeling, comprehensive structural validation, structural superimposition with the selected template, ligand-binding pocket prediction, and active-site identification.

Methods

Protein Sequence Retrieval

The amino acid sequence of *L. major* spermidine synthase (UniProt accession number Q95Z84; Gene ID: LMJF_04_0580) was retrieved from the UniProt database [27]. The complete protein sequence, consisting of 300 amino acid residues, was obtained in FASTA format and used as the input sequence for subsequent computational analyses and homology modeling [28].

Protein Sequence Analysis and Primary Structure Prediction

To characterize the physicochemical properties and primary structural features of the target protein, the ProtParam tool available through the ExPASy server was employed [29]. The molecular weight, theoretical isoelectric point (pI), atomic composition, amino acid composition, hydrophobicity index, instability index, and aliphatic index of *L. major* spermidine synthase were calculated. These parameters were used to provide information on the physicochemical characteristics and predicted stability of the target protein [29, 30].

Sequence Alignment and Homologous Sequence Analysis

The FASTA-format sequence of *L. major* spermidine synthase (Q95Z84) was compared with homologous spermidine synthase sequences from related *Leishmania* species to identify conserved regions and assess sequence similarity. Four homologous sequences from *L. infantum* (A4HS53), *L. donovani* (E9B822 and Q9GSR3), and *L. naiffi* (A0AAW3C7P9) were selected for comparative sequence analysis. The sequence similarity values of these homologous proteins ranged from 97.3% to 99.3%, as presented in Table 1. Multiple sequence alignment (MSA) was subsequently performed using Clustal Omega to identify conserved residues and sequence regions among the selected *Leishmania* homologs and the target *L. major* spermidine synthase sequence [31].

Secondary Structure Prediction

The secondary structure of *L. major* spermidine synthase was predicted using PSIPRED and GOR IV sequence analysis tools [32, 33]. These tools were used to predict the distribution of the major secondary structural elements, including alpha-helices, beta-sheets, and random coils. The percentage composition of each predicted secondary structure element was calcu-

lated to characterize the overall secondary structural organization of the protein and provide insights into its predicted folding pattern [33].

Tertiary Structure Prediction and Homology Modeling

Since no experimentally determined three-dimensional structure was available for *L. major* spermidine synthase (UniProt accession number: Q95Z84), homology modeling was performed using the SWISS-MODEL server [34]. The FASTA sequence of the target protein was submitted to the SWISS-MODEL workspace for template identification and structural model generation. Among the available experimentally determined homologous structures, the crystal structure of spermidine synthase from *T. cruzi* (PDB ID: 4YUX, chain A) was selected as the principal modeling template based on its sequence similarity to the target protein, structural relevance, and availability of a high-resolution experimentally determined structure. The selected 4YUX.1.A template structure was determined by X-ray diffraction at a resolution of 1.60 Å and represents spermidine synthase from *T. cruzi* strain CL Brener. The sequence identity between the *L. major* target protein and the selected 4YUX.1.A template was 67.92%, with approximately 88% sequence coverage. The selected template contains structurally characterized spermidine synthase with associated ligand molecules, providing a suitable structural reference for modeling the target enzyme and for subsequent analysis of ligand-binding and active-site regions. The target sequence was aligned with the selected template, followed by generation of the three-dimensional homology model using the SWISS-MODEL pipeline [34, 35]. The resulting model comprised the complete 300-amino-acid sequence of *L. major* spermidine synthase. The generated model was subsequently subjected to structural validation, quality assessment, structural comparison, binding-pocket prediction, and active-site analysis as described in the following sections.

Homology Model Validation

To assess the structural quality and stereochemical characteristics of the predicted three-dimensional structure of *L. major* spermidine synthase, several complementary in silico validation tools were employed.

1. **ERRAT** was used to evaluate the overall structural quality of the generated homology model [36]. ERRAT analyzes the statistics of non-bonded atomic interactions between different atom types and identifies regions that may contain structural errors within the modeled protein.
2. **PROCHECK** was employed to generate the Ramachandran plot and evaluate the stereochemical quality of the modeled structure by analyzing the backbone dihedral angles (φ and ψ) of amino acid residues [20]. The analysis determines the distribution of residues within the most favored, additionally allowed, generously allowed, and disallowed regions, thereby providing an assessment of the stereochemical quality of the predicted model.
3. **Verify3D** was used to evaluate the compatibility between the three-dimensional environment of the modeled protein and its amino acid sequence [37]. This analysis assesses whether individual residues occupy structural environments consistent with their physicochemical characteristics and expected three-dimensional organization.

Structural Comparison

The three-dimensional structure of *L. major* spermidine synthase generated by SWISS-MODEL was structurally compared with the selected experimentally determined template structure from the Protein Data Bank. The

4YUX.1.A structure of *T. cruzi* spermidine synthase was used as the reference structure for structural superposition and comparative analysis. The comparison was performed to assess the structural similarity between the modeled target protein and the experimentally determined homologous structure and to examine conserved structural and functional features [24].

Conserved Domain Analysis

Conserved domain analysis of *L. major* spermidine synthase was performed using the NCBI Conserved Domain Database (CDD) through the CD-Search tool [38]. The complete amino acid sequence of the target protein (Q95Z84) was submitted in FASTA format to identify conserved functional regions and domain architecture. The detected domains were evaluated according to domain identity, amino acid interval, protein classification, and statistical significance based on E-values. The resulting conserved-domain information was used to characterize the functional and evolutionary features of the target protein [39].

Model Quality Assessment Using GMQE and QMEANDisCo

The quality of the predicted three-dimensional model was further evaluated using the quality-assessment parameters provided by SWISS-MODEL. Model quality was assessed using the Global Model Quality Estimation (GMQE) and QMEANDisCo Global scores. In addition, the predicted oligomeric state and associated ligand molecules of the selected template were examined to provide additional structural context for the generated model [40].

Binding Pocket Prediction

Potential ligand-binding pockets in the homology-modeled structure of *L. major* spermidine synthase were predicted using PrankWeb based on the P2Rank machine-learning algorithm. The predicted pockets were evaluated according to their pocket scores, probabilities, number of predicted binding residues, and pocket-center coordinates. In addition, DoGSiteScorer, available through the ProteinsPlus server, was used to characterize the physicochemical properties of the predicted pockets, including pocket volume, surface area, depth, drug score, and hydrogen-bonding features. The highest-ranked pocket was subsequently considered the principal candidate ligand-binding region for further structural and active-site analysis [41].

Active Site Identification

The potential active-site region of *L. major* spermidine synthase was identified by integrating binding-pocket prediction, template-based ligand-interaction analysis, and UniProt functional annotation. The highest-ranked binding pocket predicted by PrankWeb using the P2Rank algorithm was compared with the ligand-binding region of the selected template structure (PDB ID: 4YUX), which contains S4M ligand molecules.

PyMOL was used to identify amino acid residues located within 5 Å of the template ligand. The residues identified through template-ligand interaction analysis were subsequently compared with the residues predicted to constitute Pocket 1 by PrankWeb to identify conserved ligand-binding residues. In addition, the UniProt annotation of *L. major* spermidine synthase (Q95Z84) was examined, which identifies Asp173 (D173) as a catalytic active-site residue functioning as a proton acceptor. The combined information obtained from PrankWeb, PyMOL, and UniProt was used to characterize the putative active-site region of *L. major* spermidine synthase [42].

Computational Tools and Database Resources

Various bioinformatics databases, web-based servers, and computational tools were used throughout the study for the structural and functional characterization of *L. major* spermidine synthase. The protein sequence was retrieved from the UniProt Knowledgebase (UniProtKB),

while physicochemical properties were analyzed using the ExPASy ProtParam tool. Sequence similarity analysis and multiple sequence alignment were performed using BLAST and Clustal Omega, respectively. Conserved-domain identification was conducted using the NCBI Conserved Domain Database (CDD). Homology modeling and model quality assessment were performed using the SWISS-MODEL server, while structural validation was conducted using ERRAT, PROCHECK, and Verify3D. Three-dimensional structural visualization and structural comparison were performed using PyMOL software. Binding-pocket prediction and active-site analysis were performed using PrankWeb based on the P2Rank algorithm and DoGSiteScorer through the ProteinsPlus web server [43].

Sequence Alignment and Homologous Sequence Analysis

The FASTA-format sequence of *L. major* spermidine synthase (Q95Z84) was compared with homologous spermidine synthase sequences from related *Leishmania* species to identify conserved regions and assess sequence similarity. Four homologous sequences from *Leishmania infantum* (A4HS53), *Leishmania donovani* (E9B822 and Q9GSR3), and *Leishmania naiffi* (A0AAW3C7P9) were selected for comparative sequence analysis. The sequence similarity values of these homologous proteins ranged from 97.3% to 99.3%, as presented in Table 1. Multiple sequence alignment (MSA) was subsequently performed using Clustal Omega to identify conserved residues and sequence regions among the selected *Leishmania* homologs and the target *L. major* spermidine synthase sequence [31].

Tertiary Structure Prediction and Homology Modeling

Since no experimentally determined three-dimensional structure was available for *L. major* spermidine synthase (UniProt accession number: Q95Z84), homology modeling was performed using the SWISS-MODEL server [34]. The FASTA sequence of the target protein was submitted to the SWISS-MODEL workspace for template identification and structural model generation. Among the available experimentally determined homologous structures, the crystal structure of spermidine synthase from *T. cruzi* (PDB ID: 4YUX, chain A) was selected as the principal modeling template based on its high sequence similarity to the target protein, structural relevance, and availability of a high-resolution experimentally determined structure. The selected template was determined by X-ray diffraction at a resolution of 1.60 Å and represents a spermidine synthase structure from *T. cruzi* strain CL Brener. The sequence identity between the *L. major* target protein and the selected 4YUX.1.A template was 67.92%, with approximately 88% sequence coverage. The selected template structure contains spermidine synthase in a dimeric biological assembly and includes ligand-associated structural information, providing a structurally characterized reference for modeling the target enzyme and for subsequent analysis of ligand-binding and active-site regions. The target sequence was aligned with the selected template, followed by generation of the three-dimensional homology model using the SWISS-MODEL pipeline [34, 35]. The resulting model comprised the complete 300-amino-acid sequence of *L. major* spermidine synthase. The modeled structure was subsequently subjected to independent structural validation, quality assessment, structural superposition, binding-pocket prediction, and active-site analysis as described in the following sections.

Structural Comparison

The three-dimensional (3D) structure of *L. major* spermidine synthase generated by SWISS-MODEL was compared with the selected experimentally determined template structure from the Protein Data Bank to assess structural

similarity, conserved structural features, and functional regions. The crystal structure 4YUX.1.A from *T. cruzi* spermidine synthase was used as the reference structure for structural superposition and comparative analysis [24].

Results

Primary structure Analysis

The amino acid sequence of *L. major* spermidine synthase was retrieved from the UniProt database (Accession No. Q95Z84) [44]. Sequence similarity analysis was performed using BLAST against homologous proteins from related *Leishmania* species. Four homologous sequences were identified and compared with the target sequence. The alignment results are presented in Figure 1 and Table 1 [45].

```
tr|A0AAW3C7P9|A0AAW3C7P9_9TRYP
MPGPGILSDGWFREESSMWPGQAQGLKVEKVLYDQPTEFQHLTVFESDPKGPWGTVMTLD 60
tr|Q95Z84|Q95Z84_LEIMA
MPGPGLLPDGWFREESTMWPGQAQGLKVEKVLYDQPTEFQHLTVFESDPSGPWGTVMTLD 60
tr|Q9GSR3|Q9GSR3_LEIDO
MPGPGLLPDGWFREESTMWPGQAQGLKVEKVLYDQPTEFQHLTVFESDPSGPWGTVMTLD 60
tr|A4HS53|A4HS53_LEIIN
MPGPGLLPDGWFREESTMWPGQAQGLKVEKVLYDQPTEFQHLTVFESDPSGPWGTVMTLD 60
tr|E9B822|E9B822_LEIDO
MPGPGLLPDGWFREESTMWPGQAQGLKVEKVLYDQPTEFQHLTVFESDPSGPWGTVMTLD 60
************************************************************
tr|A0AAW3C7P9|A0AAW3C7P9_9TRYP
GAIQLTDYDEFVYHEMLANLSLTCHHKPERVLVIGGGDGGVVREVLRHKSEKEGVVQSVE 120
tr|Q95Z84|Q95Z84_LEIMA
GAIQLTDYDEFVYHEMLANLSLACHHKPERVLVIGGGDGGVVREVLRHKSEKDGVVQSVE 120
tr|Q9GSR3|Q9GSR3_LEIDO
GAIQLTDYDEFVYHEMLANLSLTCHHKPERVLIIGGGDGGVVREVLRHKSEKDGIVQSVE 120
tr|A4HS53|A4HS53_LEIIN
GAIQLTDYDEFVYHEMLANLSLTCHHKPERVLIIGGGDGGVVREVLRHKSEKDGIVQSVE 120
tr|E9B822|E9B822_LEIDO
GVIQLTDYDEFVYHEMLANLSLTCHHKPERVLIIGGGDGGVVREVLRHKSEKDGIVQSVE 120
************************************************************
tr|A0AAW3C7P9|A0AAW3C7P9_9TRYP
LVDIDGAVIDQSKQHFPQIACGLANPCVTATVGDGAAFVHNAPDNVYDVVIIDTTDPEGP 180
tr|Q95Z84|Q95Z84_LEIMA
LVDIDGAVMQQSKKHFPQVACGFANPCVTATVGDGAAFVRNVPDSVYDVIIIDTTDPKGP 180
tr|Q9GSR3|Q9GSR3_LEIDO
LVDIDGAVIQQSKKHFPQIACGFANPCVTATVGDGAAFVKRAPDSVYDVIIIDTTDPKGP 180
tr|A4HS53|A4HS53_LEIIN
LVDIDGAVIQQSKKHFPQIACGFANPCVTATVGDGAAFVKRAPDSVYDVIIIDTTDPKGP 180
tr|E9B822|E9B822_LEIDO
LVDIDGAVIQQSKKHFPQIACGFANPCVTATVGDGAAFVKRAPDSVYDVIIIDTTDPKGP 180
************************************************************
tr|A0AAW3C7P9|A0AAW3C7P9_9TRYP
ASELFGAEFYKNVRRILRPGGIVCNQGESIWLHRPLIEKMMSFLKKDIGFTTVKYAMIYT 240
tr|Q95Z84|Q95Z84_LEIMA
ASELFGADFYTNVLRILRPGGVVCNQGESVWLHRPLIEKMMGFLKKDIGFATVKYAMIYI 240
tr|Q9GSR3|Q9GSR3_LEIDO
ASELFGADFYTNVLRILRPGGVLCNQGESVWLHRPLIEMMMGFLKKDIGFATVNYAMIYI 240
tr|A4HS53|A4HS53_LEIIN
ASELFGADFYTNVLRILRPGGVVCNQGESVWLHRPLIEMMMGFLKKDIGFATVKYAMIYI 240
tr|E9B822|E9B822_LEIDO
ASELFGADFYTNVLRILRPGGVVCNQGESVWLHRPLIEMMMGFLKKDIGFATVKYAMIYI 240
************************************************************
tr|A0AAW3C7P9|A0AAW3C7P9_9TRYP
PTYPCGSIGTLVCAKSVDTDLTVPRRPVESLGFADELKYYSSDMHRAAFVLPRFAAYLNE 300
tr|Q95Z84|Q95Z84_LEIMA
PTYPCGSIGTLVCAKSADTDVTVPMRPVESLGFADQLKYYSSDMHKAAFVLPRFAAHLNE 300
tr|Q9GSR3|Q9GSR3_LEIDO
PTYPCGSIGTLVCAKSADTDVTVPMRPVESLGFADQLKYYSSDMHKAAFVLPRFAAHLNE 300
tr|A4HS53|A4HS53_LEIIN
PTYPCGSIGTLVCAKSADTDVTVPMRPVESLGFADQLKYYSSDMHKAAFVLPRFAAHLNE 300
tr|E9B822|E9B822_LEIDO
PTYPCGSIGTLVCAKSADTDVTVPMRPVESLGFADQLKYYSSDMHKAAFVLPRFAAHLNE
************************************************************
```

Figure 1: The amino acid sequence used for alignment was retrieved from the UniProt database

Table 1: Accession Number, Organism, and Sequence Similarity of *L. major* Spermidine Synthase with homologous proteins

No.	*Organism*	*Accession No.*	*Protein Name*	*Sequence Similarity (%)*
1	*Leishmania infantum*	A4HS53	Putative spermidine synthase	99.3
2	*Leishmania donovani*	E9B822	Spermidine synthase	99.3
3	*Leishmania donovani*	Q9GSR3	Spermidine synthase	99.0
4	*Leishmania naiffi*	A0AAW3C7P9	Spermidine synthase tetramerization domain/Spermine	97.3

The primary structural analysis was performed using the ProtParam tool. The physicochemical properties, amino acid composition, and stability parameters of the *L. major* spermidine synthase protein are summarized in Table 2 and Table 3.

Table 2: Composition of the amino acid groups of model and template sequence

Amino acids	*Number of amino acids in the model*	*Amino acid percentage (%)*	*Number of amino acids in the template*	*Percentage of amino acids (%)*
Alanine – Ala (A)	21	7.0	16	5.4
Arginine – Arg (R)	10	3.3	15	5.1
Asparagine – Asn (N)	6	2.0	5	1.7
Aspartic acid – Asp (D)	21	7.0	23	7.8
Cysteine – Cys (C)	6	2.0	7	2.4
Glutamine – Gln (Q)	11	3.7	10	3.4
Glutamic acid – Glu (E)	16	5.3	20	6.8
Glycine – Gly (G)	28	9.3	25	8.4
Histidine – His (H)	9	3.0	10	3.4
Isoleucine – Ile (I)	12	4.0	16	5.4
Leucine – Leu (L)	24	8.0	24	8.1
Lysine – Lys (K)	15	5.0	15	5.1
Methionine – Met (M)	10	3.3	8	2.7
Phenylalanine – Phe (F)	14	4.7	13	4.4

Proline – Pro (P)	20	6.7	19	6.4
Serine – Ser (S)	15	5.0	18	6.1
Threonine – Thr (T)	16	5.3	15	5.1
Tryptophan – Trp (W)	4	1.3	4	1.4
Tyrosine – Tyr (Y)	10	3.3	9	3.0
Valine – Val (V)	32	10.7	24	8.1
Pyrrolysine – Pyl (O)	0	0.0	0	0.0
Selenocysteine – Sec (U)	0	0.0	0	0.0

Table 3: Physicochemical properties of the model and template proteins of *L. major* spermidine synthase

Properties	***Model***	***Template***
Number of amino acids	300	296
Molecular weight (Da)	32883.66	33032.59
Theoretical pI	5.16	5.21
Total number of negatively charged residues (Asp + Glu)	37	43
Total number of positively charged residues (Arg + Lys)	25	30
Total number of atoms	4594	4603
Chemical formula	C1479H2282N384O433S16	C1472H2281N395O440S15
Estimated half-life	30 hours (mammalian reticulocytes, in vitro)	30 hours (mammalian reticulocytes, in vitro)
Instability index (II)	40.25	47.49
Aliphatic index	84.73	81.62
Grand average of hydropathicity (GRAVY)	-0.046	-0.269

Secondary Structure Analysis

The secondary structure of the protein was predicted using the SOPMA protein sequence analysis software. The results for the model and template proteins, including alpha helices, coils, and extended strands, are illustrated in Figures 2–8 and Table 4. Additionally, analysis using SOPMA software indicated that the total number of amino acids is 300 for the model protein and 296 for the template protein [46].

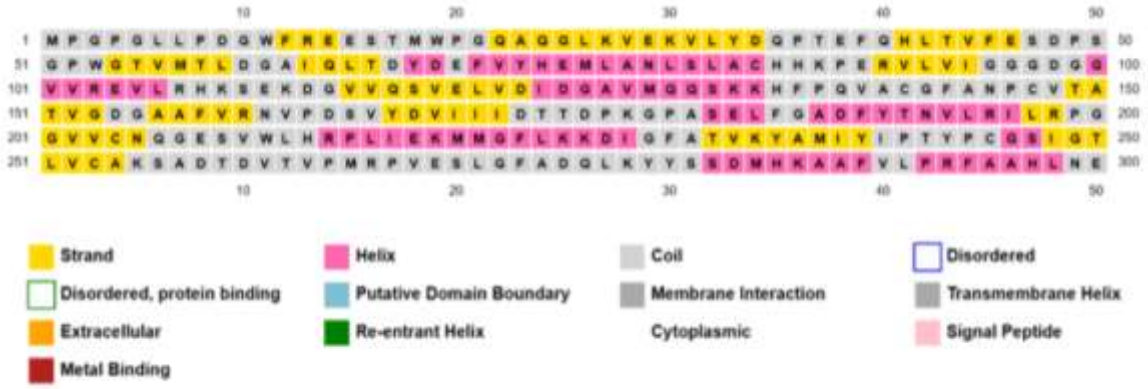


Figure 2: The model displays the presence of helices, strands, coils, turns, and loops

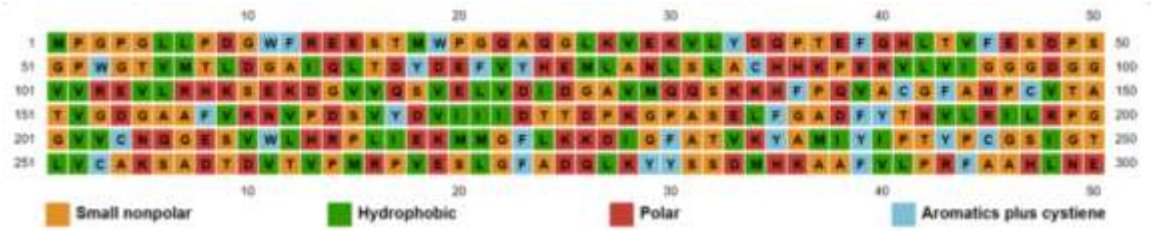


Figure 3: The model shows the presence of polar, small nonpolar, hydrophobic, aromatic plus, and cysteine residues

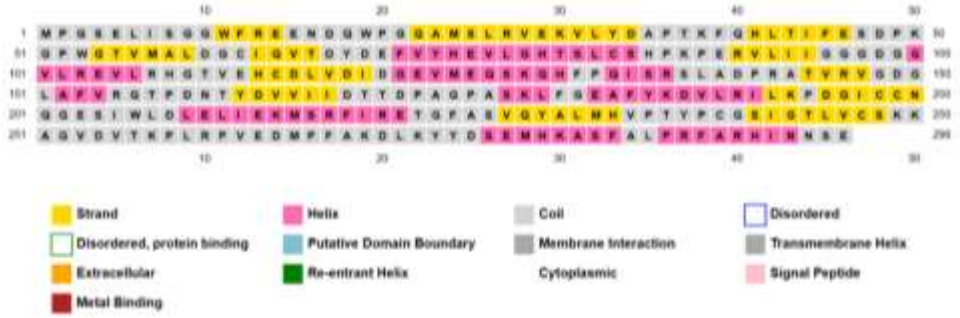


Figure 4: The template displays the presence of helices, strands, coils, turns, and loops

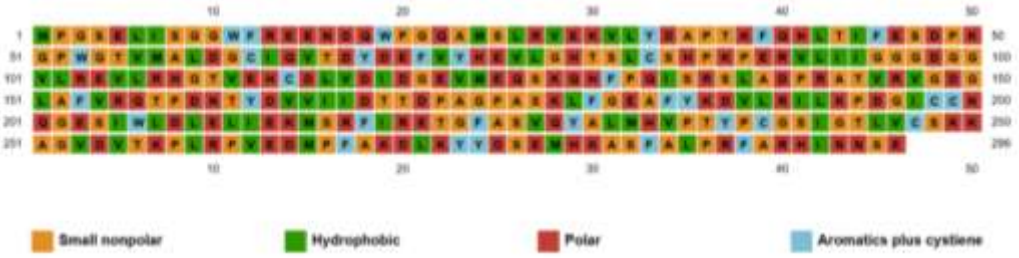


Figure 5: The template shows the presence of polar, small nonpolar, hydrophobic, aromatic plus, and cysteine residues

Table 4: Secondary structure composition of the model and template proteins

Components of the secondary structure	*Model (Q95Z84) Number*	*Model (%)*	*Template (4YUX.1.A) Number*	*Template (%)*
Alpha helix	102	34.00	101	34.12
Extended strand	59	19.67	57	19.26
Beta turn	0	0.00	0	0.00
Random coil	139	46.33	138	46.62
Total sequence length	300	100	296	100

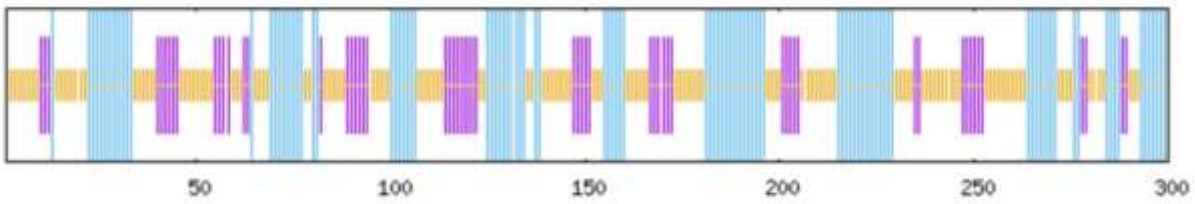


Figure 6: The secondary structure was predicted using SOPMA, which illustrates the presence of alpha helices, beta turns, extended strands, and random coils

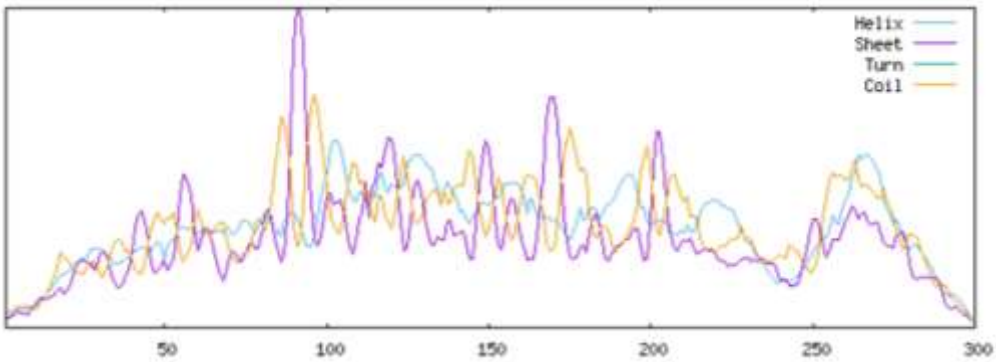


Figure 7: The secondary structure predicted by SOPMA, including alpha helices, beta turns, extended strands, and random coils, is presented in graphical form

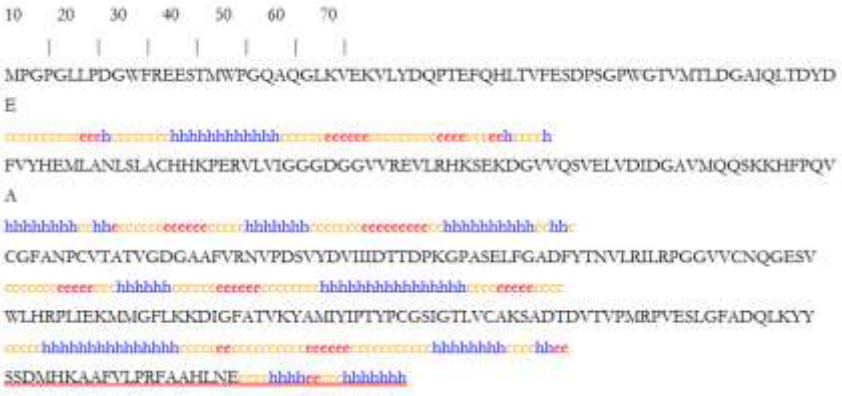


Figure 8: The secondary structure sequence predicted by SOPMA is represented using letters, where alpha helix (H), beta turn (T), random coil (C), and extended strand (E) are indicated based on these symbols

Tertiary Structure Prediction and Template Selection

The three-dimensional structure of *L. major* spermidine synthase (Q95Z84) was modeled using the SWISS-MODEL server. The four homologous sequences identified from related *Leishmania* species were used for comparative sequence analysis and multiple sequence alignment but were not used as the principal structural template for three-dimensional modeling. For homology modeling, the experimentally determined spermidine synthase structure from *T. cruzi* (PDB ID: 4YUX.1.A) was selected as the principal structural template through the SWISS-MODEL template-search workflow. Although the *Leishmania* homologous proteins showed higher sequence similarity to the target, the 4YUX.1.A structure provided an experimentally determined three-dimensional structure of spermidine synthase with a high-resolution X-ray structure (1.60 Å), approximately 88% target-template coverage, and ligand-associated structural information. Therefore, template selection was based not only on sequence similarity but also on the availability of an experimentally determined structure, target-template coverage, experimental resolution, and structural information relevant to the ligand-binding region. The resulting homology model comprised the complete 300-amino-acid sequence of *L. major* spermidine synthase. The target-template alignment showed 67.92% sequence identity and approximately 88% coverage, while the selected template had an experimental resolution of 1.60 Å (Table 5) [47].

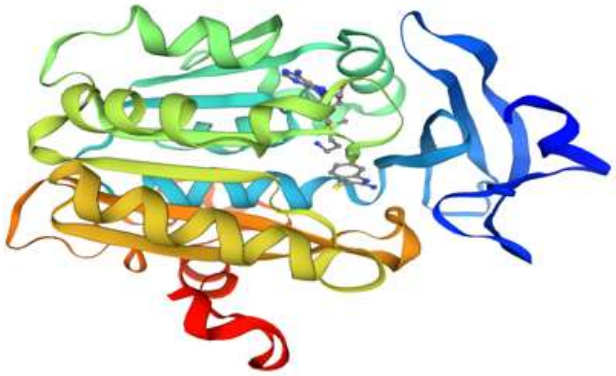


Figure 9: Three-dimensional structure of the experimentally determined *Trypanosoma cruzi* spermidine synthase (PDB ID: 4YUX.1.A) used as the principal structural template for homology modeling of *L. major* spermidine synthase

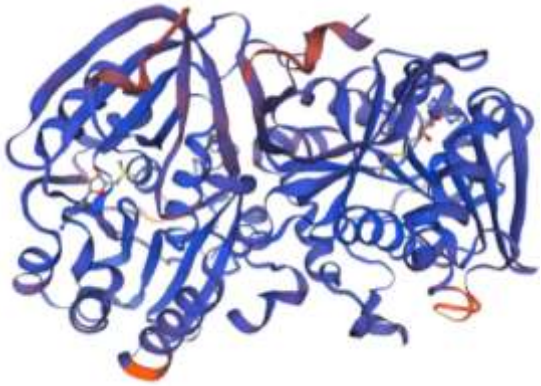


Figure 10: Three-dimensional homology model of *L. major* spermidine synthase (UniProt Q95Z84) generated using the SWISS-MODEL server with *Trypanosoma cruzi* spermidine synthase (4YUX.1.A) as the principal structural template

Homology Modelling Validation

The predicted three-dimensional model of *L. major* spermidine synthase (Q95Z84), in PDB file format, was evaluated using the ERRAT tool [48]. The PROCHECK tool was used to generate the Ramachandran plot [49], and the Verify3D tool was employed to assess the compatibility of the three-dimensional model with its amino acid sequence [50]. The results of these structural assessment procedures are illustrated in Figures 11-13.

Structural Comparison

The three-dimensional structure of *L. major* spermidine synthase generated using the 4YUX.1.A template was structurally compared with the experimentally determined *T. cruzi* spermidine synthase structure. The target-template alignment showed 67.92% sequence identity with approximately 88% coverage, and the selected template had an experimental resolution of 1.60 Å (Table 5). The structural comparison was used to examine the correspondence between the modeled target structure and the experimentally determined reference structure and to identify conserved structural features [51].

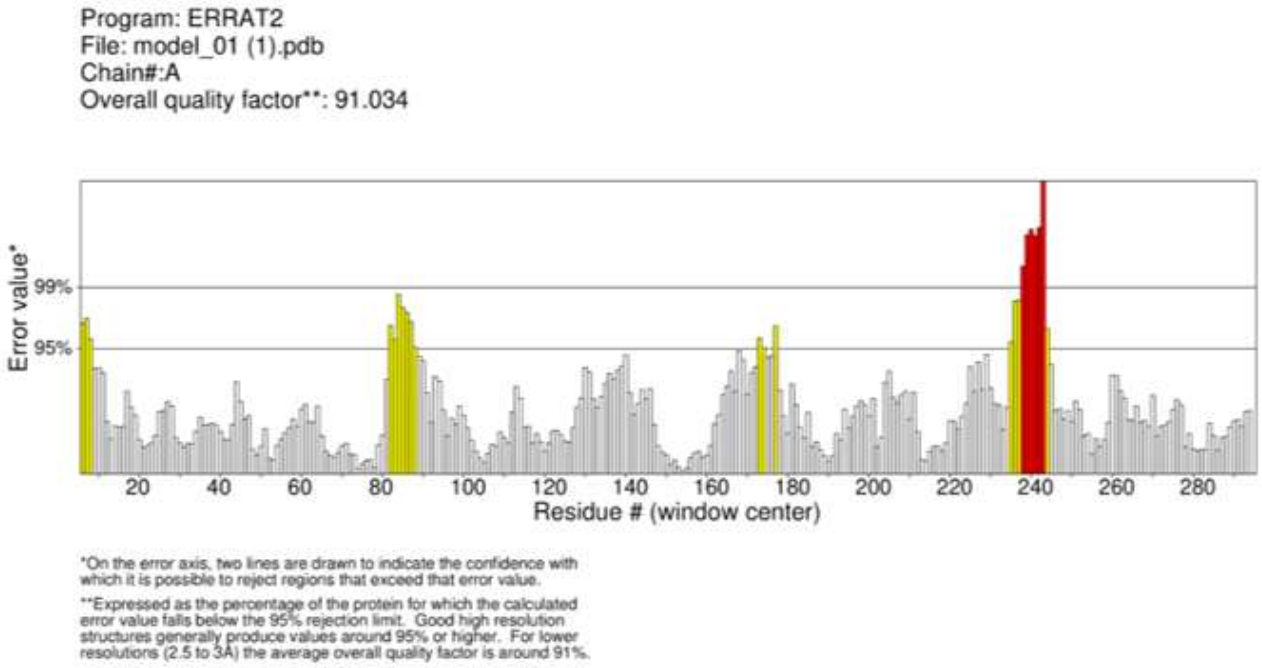


Figure 11: Structural validation was performed using ERRAT. Two reference lines were drawn to high light regions that are likely to be rejected due to having error values exceeding the acceptable threshold

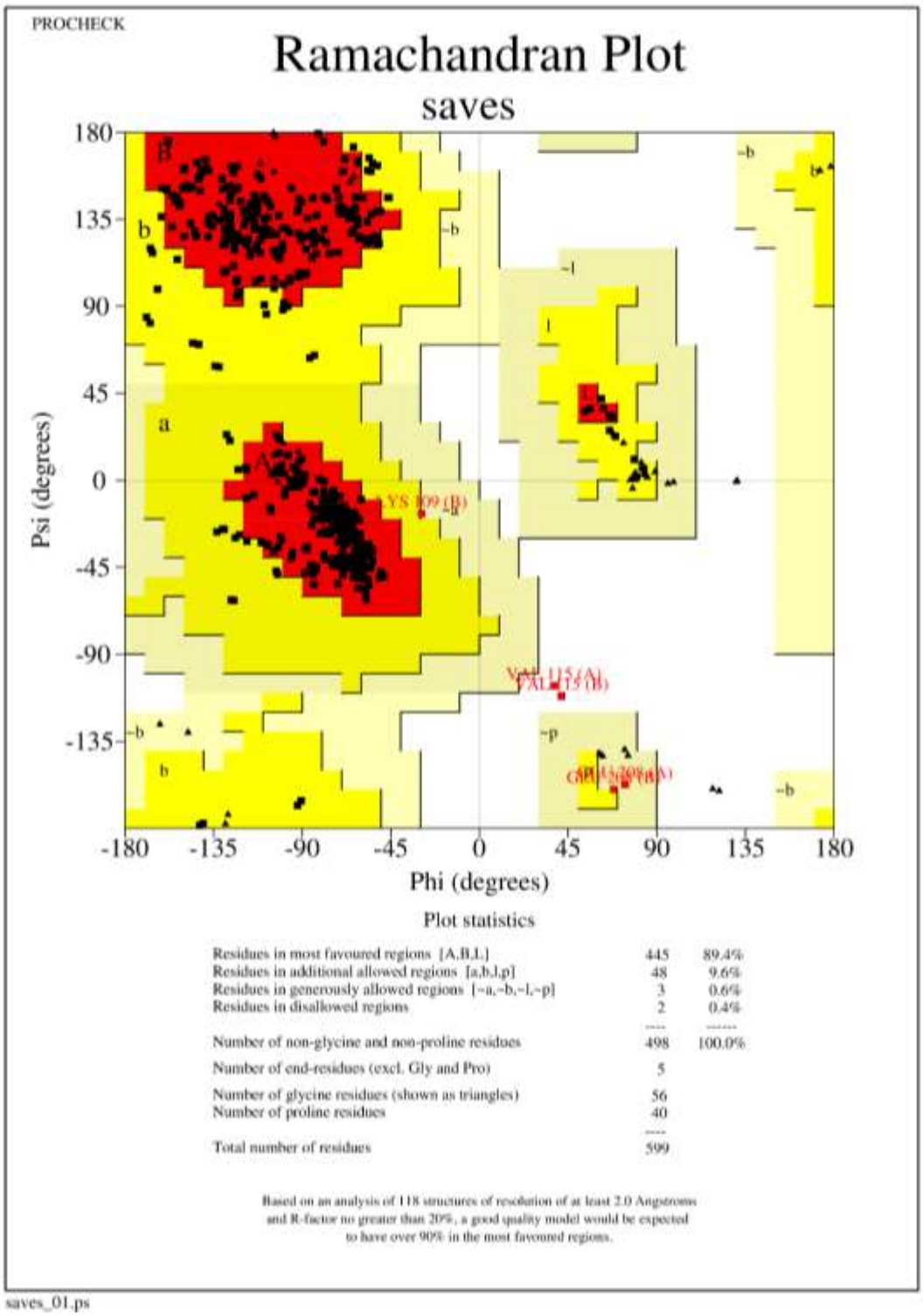


Figure 12: The structural validity of the L4MO enzyme model was assessed using a Ramachandran plot, which displays the distribution of psi–phi angle probabilities

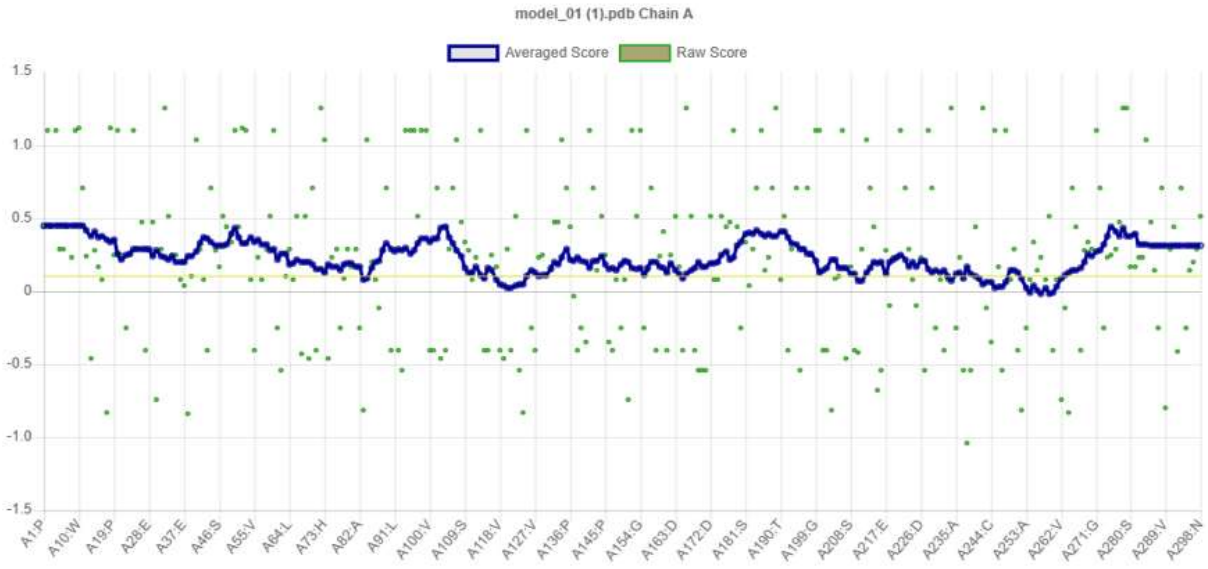


Figure 13: The atomic 3D model of *L. major* Spermidine Synthase was validated against the complete amino acid (1D) sequence using the Verify3D tool to ensure model reliability.

Table 5: Structural comparison between predicted model and template

Parameter	***Result***
Target protein	*L. major* Spermidine Synthase
Template	4YUX.1.A
Template protein	*Trypanosoma cruzi* Spermidine synthase
Sequence identity	67.92%
Coverage	0.88
Template resolution	1.6 Å

Conserved Domain Analysis

The conserved domain analysis identified a spermidine synthase domain (PLN02366) covering amino acid positions 9–295 with a highly significant E-value (2.14×10^{-100}), confirming the conserved functional region of the *L. major* Spermidine Synthase protein in table 6 and Figure 14.

Table 6: Conserved domain analysis of *L. major* Spermidine Synthase using NCBI CDD

Protein	***Conserved domain***	***Superfamily classification***	***Domain interval***	***E-value***
L. major Spermidine Synthase (Q95Z84)	Spermidine synthase (PLN02366)	Class I SAM-dependent methyltransferase (ArchID: 106779)	9–295 aa	2.14×10^{-100}

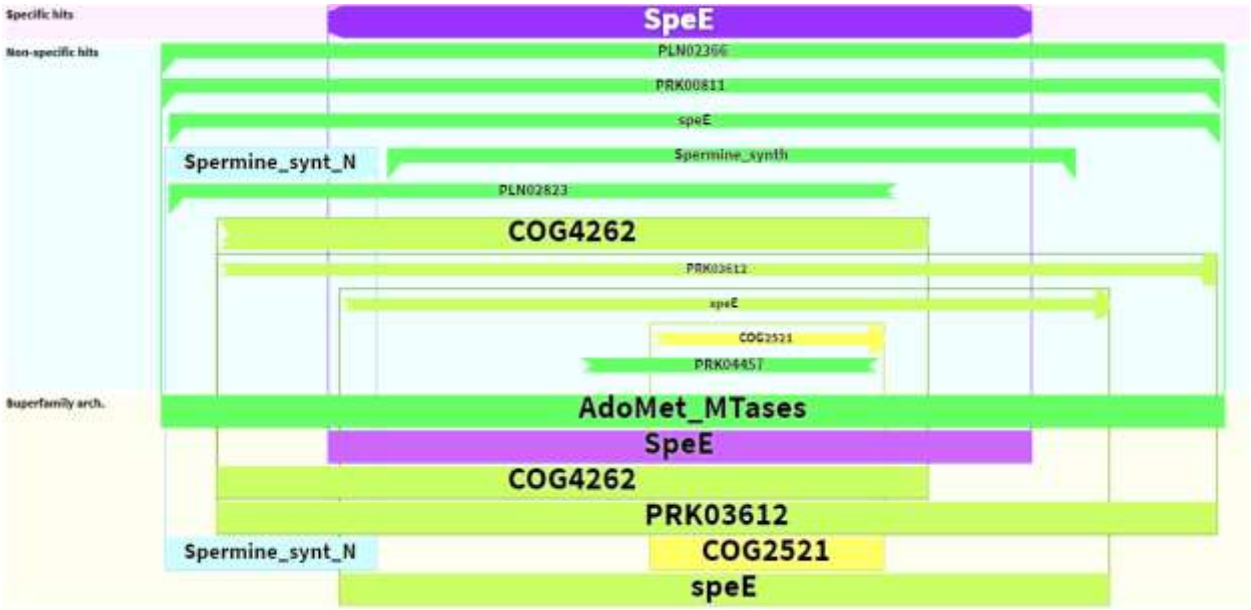


Figure 14. Conserved domain architecture of *L. major* Spermidine Synthase identified using the NCBI Conserved Domain Database (CDD).

Model Quality Assessment Using GMQE and QMEANDisCo

The generated *L. major* spermidine synthase model obtained a Global Model Quality Estimation (GMQE) score of 0.87 and a QMEANDisCo Global score of 0.83 ± 0.05 (Table 7). These model-quality estimates were interpreted together with the 67.92% target-template sequence identity, approximately 88% sequence coverage, and the 1.60 Å experimental resolution of the selected 4YUX.1.A template (Table 5). GMQE and QMEANDisCo were considered complementary estimates of the expected quality of the generated model and were not treated as independent experimental validation measures.

Table 7: Quality assessment parameters of the predicted model

Parameter	***Value***
GMQE	0.87
QMEANDisCo Global	0.83 ± 0.05
Oligomeric state	Template-derived dimeric assembly
Ligands	2 × S4M (template-associated)

The SWISS-MODEL output reported a dimeric assembly for the modeled protein, corresponding to the oligomeric organization of the selected 4YUX.1.A template. Therefore, the reported homo-dimeric state represents a template-derived structural assignment rather than an independent experimental determination of the oligomeric state of *L. major* spermidine synthase. The selected 4YUX.1.A structure also contains two S4M ligand-associated molecules, which were considered as structural reference information for subsequent analysis of the ligand-binding and active-site regions.

Binding Pocket Prediction

PrankWeb analysis identified three potential ligand-binding pockets within the modeled structure of **L . major** Spermidine Synthase. Among the predicted pockets, Pocket 1 showed the highest prediction score (24.37) and probability (0.898), suggesting it as the most probable ligand-binding region. Therefore, Pocket 1 was selected for further structural characterization in Table 8.

Table8: Predicted ligand-binding pockets identified by PrankWeb

Pocket	*Rank*	*Score*	*Probability*	*Number of Residues*	*Pocket Center (X,Y,Z)*
Pocket 1	1	24.37	0.898	34	(5.1566, 9.5048, 41.9166)
Pocket 2	2	24.02	0.895	33	(-8.2907, 5.7887, 8.9473)
Pocket 3	3	5.50	0.262	13	(-9.6571, -20.3335, 7.3739)

DoGSiteScorer Analysis of Pocket 1

The physicochemical properties of Pocket 1 were further analyzed using DoGSiteScorer. The selected pocket showed favorable structural characteristics with a volume of **931.34 Å³**, surface area of **905.37 Å²**, and a drug score of 0.83, supporting its characterization as a potential ligand-binding region (Table 9).

Table 9: Physicochemical properties of the selected binding pocket (P_1)

sProperty	*Value*
Pocket Volume	931.34 Å³
Surface Area	905.37 Å²
Drug Score	0.83
Simple Score	0.53
Depth	25.96 Å
Pocket Atoms	241
Hydrogen Bond Donors	21
Hydrogen Bond Acceptors	74
Hydrophobic Interactions	26
Hydrophobicity Ratio	0.21

Active Site Identification

Comparison of the highest-ranked PrankWeb Pocket 1 with the ligand-associated region of the experimentally determined 4YUX.1.A template was used to identify residues surrounding the putative ligand-binding region of *L. major* spermidine synthase. The two S4M ligand-associated molecules in the template structure provided structural reference coordinates for mapping the corresponding ligand-binding region onto the modeled protein. Residues identified around the template-associated ligand region were compared with the residues predicted to constitute Pocket 1 by PrankWeb in Figure 15,16. The ligand-associated structural information was used as a reference for localization of the putative ligand-binding region and was not interpreted as experimental evidence that S4M binds to the modeled *L. major* enzyme in Figure 17. In addition, UniProt functional annotation (Q95Z84) identifies Asp173 (D173) as a catalytic active-site residue functioning as a proton acceptor. The integration of template-associated ligand information, predicted pocket residues, and UniProt functional annotation provided complementary information for defining the putative active-site region of the modeled enzyme. The conserved residues associated with the binding pocket are summarized in Table 10.

Table 10: Conserved binding pocket-associated residues

No.	*Common Active Site Residues*
1	GLN40
2	LEU59
3	GLN64
4	TYR73
5	HIS74
6	GLY95
7	PRO175
8	ASP98
9	VAL123
10	GLY96
11	THR175

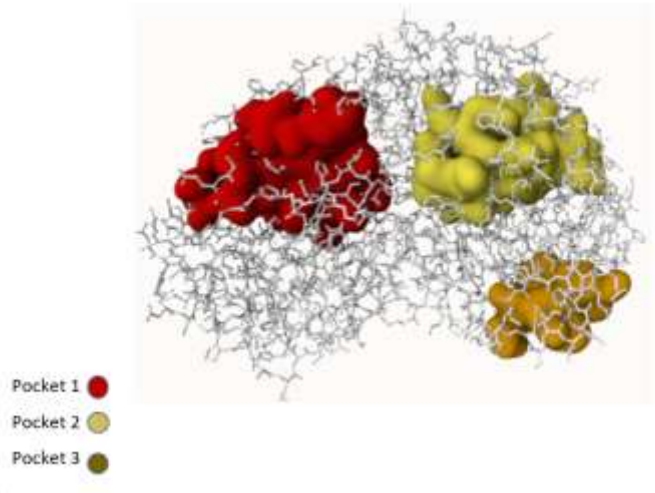


Figure 15: Predicted ligand-binding pockets of *L. major* Spermidine Synthase identified by PrankWeb (P2Rank algorithm). Three potential pockets (P1–P3) were detected in the modeled structure

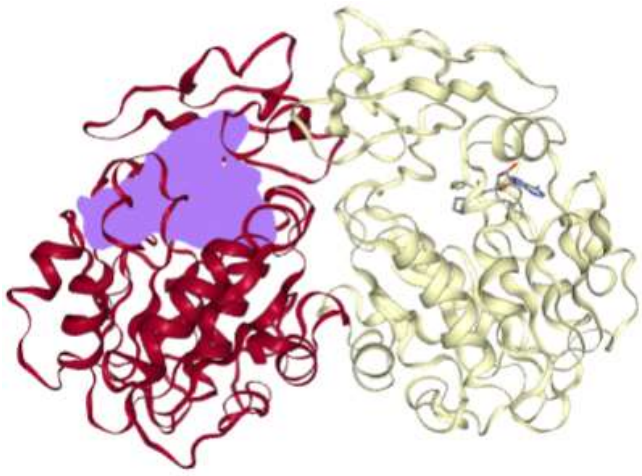


Figure 16: Three-dimensional visualization of the highest-ranked binding pocket (P_1) of *L. major* Spermidine Synthase predicted by DoGSiteScorer, showing favorable ligand-binding properties

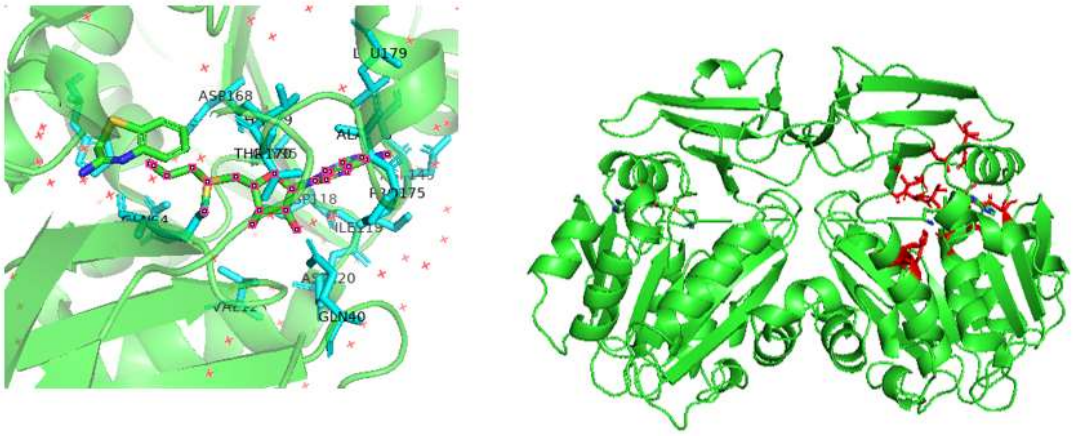


Figure 17: Three-dimensional visualization of the putative active-site region of *L. major* spermidine synthase based on S4M ligand-associated structural information from the 4YUX.1.A template and the UniProt-annotated catalytic residue Asp173. The highlighted residues represent residues associated with the predicted ligand-binding region

Discussion

The present study provides an integrated in silico structural characterization of *L. major* SPDS, combining sequence analysis, physicochemical profiling, secondary- and tertiary-structure prediction, homology-model validation, conserved-domain analysis, structural comparison, and ligand-binding pocket prediction. Spermidine is an important component of polyamine metabolism in *Leishmania* and serves as a precursor for trypanothione, a major redox-related metabolite in trypanosomatid parasites. The importance of polyamine and trypanothione metabolism in parasite growth, survival, and oxidative-stress management has made enzymes of these pathways relevant targets for antileishmanial drug-discovery research [53, 55]. However, because spermidine synthase is also present in humans, the therapeutic relevance of *L. major* SPDS should be considered in terms of parasite–host structural differences rather than being attributed solely to the parasite-specific nature of the downstream trypanothione pathway [54,55].

The primary sequence analysis demonstrated that the 300-amino-acid *L. major* SPDS shares high sequence similarity with homologous SPDS proteins from other *Leishmania* species. The observed sequence similarity ranged from 97.3% to 99.3% for *L. naiffi*, *L. donovani*, and *L. infantum*, respectively. The multiple-sequence alignment further demonstrated extensive conservation throughout the protein sequence, supporting the evolutionary conservation of SPDS within the examined *Leishmania* species. Such conservation indicates that the overall structural organization of SPDS is likely to be maintained among these species. Nevertheless, overall sequence identity alone does not establish conservation of every functionally important residue or guarantee that an inhibitor developed against one ortholog will exhibit equivalent activity against another. Therefore, residue-level conservation of the catalytic and proposed ligand-binding regions is more informative when considering the possible cross-species relevance of SPDS-targeted inhibitors [45, 56].

The physicochemical analysis showed a theoretical pI of 5.16, with 37 negatively charged residues and 25 positively charged residues. The negative GRAVY value (-0.046) indicates a slightly hydrophilic character, whereas the aliphatic index of 84.73 suggests a substantial contribution of aliphatic residues to the protein

sequence. The predicted secondary structure consisted of 34.00% alpha-helices, 19.67% extended strands, and 46.33% random coils. The broadly similar secondary-structure composition between the modeled protein and the selected template supports the preservation of the general structural framework observed in the reference spermidine synthase.

An important point concerns the ProtParam instability index. The calculated instability index of the *L. major* SPDS was 40.25. Because ProtParam uses a value below 40 as the threshold for a protein predicted to be stable and values above 40 as indicative of possible instability, 40.25 should not be described as evidence of a stable protein . Instead, this value represents a borderline or slightly elevated instability prediction. Importantly, the instability index is a sequence-based statistical prediction and should not be interpreted as direct experimental evidence of protein stability under physiological conditions. Accordingly, the present value should be considered cautiously and independently from the structural-quality assessments of the homology model.

The selection of *Trypanosoma cruzi* SPDS (PDB ID: 4YUX.1.A) as the principal structural template was supported by several complementary criteria. Although the *Leishmania* homologs used for sequence analysis exhibited higher sequence similarity to the target, 4YUX.1.A provided an experimentally determined three-dimensional structure with 67.92% sequence identity to the target, approximately 88% coverage, and a high experimental resolution of 1.60 Å. The availability of ligand-associated structural information additionally made this experimentally characterized structure useful for investigating the putative ligand-binding region of *L. major* SPDS.

The resulting model showed favorable computational quality estimates, including a GMQE score of 0.87 and a QMEANDisCo Global score of 0.83 ± 0.05. These values, together with the high target-template sequence identity and substantial sequence coverage, support the use of the predicted structure as a structural hypothesis for subsequent computational analysis. Structural validation further yielded an ERRAT quality factor of 91.034% and a Ramachandran analysis in which 99.0% of residues were located within the favored and additionally allowed regions [48, 50]. The Verify3D analysis also supported compatibility between the predicted three-dimensional environment and the amino-acid sequence. Collectively, these results indicate that the model has a suitable computational quality for exploratory structural and ligand-binding analyses.

Nevertheless, these validation metrics should not be interpreted as experimental confirmation of the structure. The modeled dimeric organization and the presence of two S4M molecules were derived from the template-associated structural information and therefore represent template-informed structural assignments rather than experimentally demonstrated properties of *L. major* SPDS. This distinction is particularly important when interpreting subsequent active-site and ligand-binding analyses.

Conserved-domain analysis identified the spermidine synthase domain PLN02366 spanning residues 9–295, with a highly significant E-value of 2.14×10^{-100}. This result provides strong sequence-based support for the assignment of the modeled protein as a spermidine synthase and indicates that the majority of the 300-residue sequence belongs to a conserved functional domain. The agreement between the domain-level annotation, the structural model, and the known biological role of spermidine synthase strengthens the functional interpretation of the predicted structure.

PrankWeb identified three potential ligand-binding pockets, with Pocket 1 showing the highest prediction score (24.37) and probability (0.898). DoGSiteScorer further characterized Pocket 1 as a relatively substantial cavity with a volume of 931.34 $Å^3$, surface area of 905.37 $Å^2$, depth of 25.96 Å, and a drug score of 0.83.

These characteristics support the classification of Pocket 1 as a potentially ligandable region. However, the drug score should be interpreted as an indicator of pocket physicochemical suitability rather than direct evidence that a compound will bind with high affinity. Experimental binding measurements would ultimately be required to establish ligand affinity.

The integration of the PrankWeb prediction with the ligand-associated region of the 4YUX.1.A template provided a structural basis for defining the putative active-site region. Eleven residues were identified around the proposed binding region: GLN40, LEU59, GLN64, TYR73, HIS74, GLY95, GLY96, ASP98, VAL123, PRO175, and THR175, while UniProt functional annotation independently identifies Asp173 as a catalytic residue functioning as a proton acceptor. These findings provide complementary computational and annotation-based evidence for the localization of a functionally relevant region in the modeled enzyme. However, because the pocket residues were inferred computationally and the S4M molecules originate from the template structure, these residues should be regarded as proposed ligand-binding/active-site-associated residues rather than experimentally confirmed inhibitor-contact residues.

The high overall sequence similarity among the analyzed *Leishmania* SPDS proteins provides evidence for strong evolutionary conservation of the enzyme. Inspection of the multiple-sequence alignment demonstrates that many regions surrounding the proposed functional architecture are highly conserved. This conservation is consistent with the central metabolic role of spermidine synthesis in trypanosomatids. However, overall sequence similarity should not by itself be used to claim broad-spectrum inhibitor efficacy. The pharmacological relevance of the present findings therefore depends on whether the specific catalytic residue and proposed pocket-associated residues are conserved at the corresponding positions across the examined orthologs [54, 56].

In the present dataset, the alignment provides the basis for evaluating residue-level conservation across *L. infantum*, *L. donovani*, and *L. naiffi*. The catalytic Asp173 and the proposed pocket-associated residues should therefore be interpreted according to their residue-specific alignment rather than solely according to the reported 97.3–99.3% overall sequence similarity. Where these residues are conserved, the conservation supports the possibility that the corresponding structural region is maintained among the examined species; where substitutions occur, such differences may instead contribute to species-specific recognition. Thus, the present findings support conservation of the SPDS scaffold but do not, on their own, establish equivalent inhibitor susceptibility across all *Leishmania* species.

An important consideration in interpreting SPDS as a therapeutic target is that humans also possess a functional spermidine synthase. Consequently, the parasite-specific nature of the downstream trypanothione pathway cannot alone establish selective inhibition of *L. major* SPDS or minimal host toxicity. The present study provides a structural framework for identifying the parasite enzyme's putative ligand-binding region, but it does not include a direct structural alignment or residue-level comparison with human spermidine synthase. Therefore, selective inhibition should be regarded as a hypothesis generated by the present structural analysis rather than a demonstrated property of the modeled enzyme [57].

The predicted pocket and its associated residues may provide a starting point for future comparative analysis with human SPDS. In particular, residues that differ between the parasite and human enzymes within or immediately surrounding the ligand-binding region could represent candidate determinants for parasite-preferential recognition. Such a comparison, followed by docking of candidate compounds

against both parasite and human SPDS and subsequent experimental testing, would be necessary to substantiate claims regarding selectivity and host toxicity. This distinction is important because structural similarity between host and parasite metabolic enzymes can present a challenge for selective inhibitor design [53, 55].

Several limitations should be considered when interpreting the present findings. First, the *L. major* SPDS structure was generated by homology modeling rather than determined experimentally. Although the model showed favorable sequence-based and stereochemical quality metrics, static computational models cannot fully represent conformational flexibility, solvent effects, side-chain rearrangements, or transient states that may influence ligand recognition. Second, the binding pocket was predicted computationally, and the S4M-associated structural information was derived from the template rather than experimentally demonstrated for *L. major* SPDS. Third, no molecular docking, molecular dynamics simulation, binding free-energy calculation, biochemical inhibition assay, or cellular validation was performed in the present study [58].

Molecular dynamics simulations would therefore be valuable as a subsequent step to evaluate the stability and flexibility of the predicted pocket, the persistence of residue interactions, and possible conformational changes during ligand binding. Comparative docking and, where appropriate, longer-timescale MD simulations against both *L. major* and human SPDS could further investigate the structural basis of parasite-preferential recognition. Ultimately, biochemical enzyme-inhibition experiments and cellular assays would be required to determine whether compounds predicted to interact with the identified pocket actually inhibit SPDS activity and whether such inhibition translates into antileishmanial effects without unacceptable host toxicity [59]. Thus, the current model should be considered a structural hypothesis and a foundation for subsequent experimental and dynamic computational investigations rather than definitive evidence of drug efficacy.

Overall, this study establishes a computational structural framework for *L. major* spermidine synthase by integrating sequence conservation, physicochemical characterization, homology modeling, structural validation, conserved-domain analysis, and complementary binding-pocket prediction. The high sequence conservation among the examined *Leishmania* SPDS proteins and the favorable quality of the modeled structure support further investigation of this enzyme as a candidate target within parasite polyamine metabolism [60]. The identification of a high-ranking putative ligand-binding pocket and associated residues provides a rational structural starting point for future inhibitor-design studies. Nevertheless, the therapeutic significance of these findings should be interpreted cautiously because host SPDS is also present and the current study does not experimentally establish parasite selectivity, ligand affinity, or biological efficacy. Future comparative structural analyses, molecular dynamics simulations, biochemical assays, and cellular validation will therefore be essential for determining whether the structural features identified here can be translated into selective antileishmanial intervention strategies.

Conclusion

This study provides an integrated in silico structural characterization of *L. major* SPDS, an enzyme involved in polyamine metabolism and indirectly linked to trypanothione biosynthesis. Sequence analysis revealed high conservation among *Leishmania* SPDS homologs, with 97.3–99.3% identity across the examined species. Homology modeling using the experimentally determined *Trypanosoma cruzi* SPDS structure (PDB ID: 4YUX) generated a structurally plausible model supported by favorable GMQE, QMEANDisCo, ERRAT, Ramachandran, and Verify3D assessments. Conserved-domain

analysis and complementary pocket-prediction tools identified a putative ligand-binding region that may guide future structural and functional investigations. However, the predicted pocket, catalytic-site assignments, and template-informed structural features remain computational hypotheses requiring experimental confirmation. Because SPDS is also present in humans, the potential for parasite-selective inhibition cannot be inferred from sequence conservation or pathway differences alone. Comparative structural analyses of parasite and human SPDS, followed by molecular simulations, biochemical inhibition assays, and cellular validation, are needed to assess selectivity and therapeutic potential. Overall, this study establishes a useful structural framework for investigating *L. major* SPDS and prioritizing candidates for future antileishmanial drug-discovery research, without claiming demonstrated inhibitor efficacy or parasite selectivity.

Conflicts of interest

The authors declare no conflicts of interest, financial or otherwise, that could have influenced the work reported in this study.

Funding

This research received no specific grant from any funding agency in the public, commercial, or not-for-profit sectors.

Ethical Considerations

This study was based on in silico computational analyses of protein sequence and structural data. It did not involve human participants, animal experiments, or the collection of personal or clinical data. Therefore, ethical approval and informed consent were not applicable.

Declaration of AI-Assisted Writing

The authors used ChatGPT (OpenAI) solely for language editing and grammatical improvement. The AI tool was not used to generate scientific data, perform data analysis, interpret research findings, or draw scientific conclusions. The authors reviewed and approved the final manuscript and take full responsibility for its content.

Acknowledgments

The author gratefully acknowledges the Department of Chemistry, Faculty of Science, Nangarhar University, Afghanistan, and Spinghar University, Kabul, Afghanistan, for their academic support and institutional contributions.

References

1. Burza S, Croft SL, Boelaert M. Leishmaniasis. Lancet. 2018;392(10151):951–70.
2. Alvar J, Vélez ID, Bern C, Herrero M, Desjeux P, Cano J, et al. Leishmaniasis worldwide and global estimates of its incidence. PLoS One. 2012;7(5):e35671.
3. World Health Organization. Leishmaniasis [Internet]. World Health Organization; 2023 Jan 12 [cited 2026 Nov 8]. Available from: https://www.who.int/news-room/fact-sheets/detail/leishmaniasis
4. Reguera RM, Pérez-Pertejo Y, Gutiérrez-Corbo C, Domínguez-Asenjo B, Ordóñez C, García-Estrada C, et al. Current and promising novel drug candidates against visceral leishmaniasis. Pure Appl Chem. 2019;91(8):1385–404.
5. Dufe VT, Ingner D, Heby O, Khomutov AR, Persson L, Al-Karadaghi S. A structural insight into the inhibition of human and *Leishmania donovani* ornithine decarboxylases by 1-aminooxy-3-aminopropane. Biochem J. 2007;405(2):261–8.
6. Singh S, Sarma S, Katiyar SP, Das M, Bhardwaj R, Sundar D, et al. Probing the molecular mechanism of hypericin-induced parasite death pro-

vides insight into the role of spermidine beyond redox metabolism in *Leishmania donovani*. Antimicrob Agents Chemother. 2015;59(1):15–24.
7. Melcon-Fernandez E, Galli G, García-Estrada C, Balaña-Fouce R, Reguera RM, Pérez-Pertejo Y. Miltefosine and nifuratel combination: a promising therapy for the treatment of *Leishmania donovani* visceral leishmaniasis. Int J Mol Sci. 2023;24(2):1635.
8. Roberts SC, Jiang Y, Gasteier J, Frydman B, Marton LJ, Heby O, et al. *Leishmania donovani* polyamine biosynthetic enzyme overproducers as tools to investigate the mode of action of cytotoxic polyamine analogs. Antimicrob Agents Chemother. 2007;51(2):438–45.
9. Hubin TJ, Walker AN, Davilla DJ, Carder Freeman TN, Epley BM, Hasley TR, et al. Tetraazamacrocyclic derivatives and their metal complexes as antileishmanial leads. Polyhedron. 2019;163:42–53.
10. Wadanambi P. Computational approach to identify potential antileishmanial activity of reported inhibitor, E5700 and two natural alkaloids against *Leishmania donovani* Squalene Synthase. Exp Results. 2020;1:e31.
11. Croft SL, Sundar S, Fairlamb AH. Drug resistance in leishmaniasis. Clin Microbiol Rev. 2006;19(1):111–26.
12. Sundar S, Singh A. Recent developments and future prospects in the treatment of visceral leishmaniasis. Ther Adv Infect Dis. 2016;3(3–4):98–109.
13. Ouellette M, Drummelsmith J, Papadopoulou B. Leishmaniasis: drugs in the clinic, resistance and new developments. Drug Resist Updat. 2004;7(4–5):257–66.
14. Fairlamb AH, Cerami A. Metabolism and functions of trypanothione in the Kinetoplastida. Annu Rev Microbiol. 1992;46:695–729.
15. Müller S, Liebau E, Walter RD, Krauth-Siegel RL. Thiol-based redox metabolism of protozoan parasites. Trends Parasitol. 2003;19(7):320–8.
16. Tabor CW, Tabor H. Polyamines. Annu Rev Biochem. 1984;53:749–90.
17. Pegg AE. Mammalian polyamine metabolism and function. IUBMB Life. 2009;61(9):880–94.
18. Roberts SC, Jiang Y, Jardim A, Carter NS, Heby O, Ullman B. Genetic analysis of spermidine synthase from *Leishmania donovani*. Mol Biochem Parasitol. 2001;115(2):217–26.
19. Ilari A, Fiorillo A, Baiocco P, Poser E, Angiulli G, Colotti G. Targeting polyamine metabolism for finding new drugs against leishmaniasis: a review. Mini Rev Med Chem. 2015;15(3):243–52.
20. Heby O, Roberts SC, Ullman B. Polyamine biosynthetic enzymes as drug targets in parasitic protozoa. Biochem Soc Trans. 2003;31(2):415–9.
21. Boitz JM, Yates PA, Kline C, Gaur U, Wilson ME, Ullman B, et al. *Leishmania donovani* ornithine decarboxylase is indispensable for parasite survival in the mammalian host. Infect Immun. 2009;77(2):756–63.
22. Willert EK, Phillips MA. Regulated expression of an essential allosteric activator of polyamine biosynthesis in African trypanosomes. PLoS Pathog. 2008;4(10):e1000183.
23. Carter NS, Kawasaki Y, Nahata SS, Elikaee S, Rajab S, Salam L, et al. Polyamine metabolism in *Leishmania* parasites: a promising therapeutic target. Med Sci (Basel). 2022;10(2):24.
24. Gilroy C, Olenyik T, Roberts SC, Ullman B. Spermidine synthase is required for virulence of *Leishmania donovani*. Infect Immun. 2011;79(7):2764–9.
25. Birkholtz LM, Williams M, Niemand J, Louw AI, Persson L, Heby O. Polyamine homoeostasis as a drug target in pathogenic protozoa: peculiarities and possibilities. Biochem J. 2011;438(2):229–44.
26. Roberts SC, Scott J, Gasteier JE, Jiang Y, Brooks B, Jardim A, et al. S-adenosylmethionine decarboxylase from *Leishmania donovani*. Molecular, genetic, and biochemical characterization of null mutants and overproducers. J Biol Chem. 2002;277(8):5902–9.
27. Gasteiger E, Hoogland C, Gattiker A, Duvaud S, Wilkins MR, Appel RD, et al. Protein identification and analysis tools on the ExPASy server. In: Walker JM, editor. The proteomics protocols handbook. Totowa: Humana Press; 2005. p. 571–607.
28. Jones DT. Protein secondary structure prediction based on position-specific scoring matrices. J Mol Biol. 1999;292(2):195–202.
29. Geourjon C, Deléage G. SOPMA: significant improvements in protein secondary structure prediction by consensus prediction from multiple

alignments. Comput Appl Biosci. 1995;11(6):681–4.
30. Sievers F, Wilm A, Dineen D, Gibson TJ, Karplus K, Li W, et al. Fast, scalable generation of high-quality protein multiple sequence alignments using Clustal Omega. Mol Syst Biol. 2011;7:539.
31. McGuffin LJ, Bryson K, Jones DT. The PSIPRED protein structure prediction server. Bioinformatics. 2000;16(4):404–5.
32. Garnier J, Gibrat JF, Robson B. GOR method for predicting protein secondary structure from amino acid sequence. Methods Enzymol. 1996;266:540–53.
33. Waterhouse A, Bertoni M, Bienert S, Studer G, Tauriello G, Gumienny R, et al. SWISS-MODEL: homology modelling of protein structures and complexes. Nucleic Acids Res. 2018;46(W1):W296–303.
34. Colovos C, Yeates TO. Verification of protein structures: patterns of nonbonded atomic interactions. Protein Sci. 1993;2(9):1511–9.
35. Laskowski RA, MacArthur MW, Moss DS, Thornton JM. PROCHECK: a program to check the stereochemical quality of protein structures. J Appl Crystallogr. 1993;26(2):283–91.
36. Haqmal, A., Momand, Z. K., & Aftab, S. (2026). Structural modeling of Luciferin 4-Monooxygenase from Human Respiratory Syncytial Virus using homology techniques. Spinghar Journal of Biomedical Science, 2(1), 80–95. https://doi.org/10.64444/sjbs.21.
37. Benkert P, Biasini M, Schwede T. Toward the estimation of the absolute quality of individual protein structure models. Bioinformatics. 2011;27(3):343–50.
38. Marchler-Bauer A, Derbyshire MK, Gonzales NR, Lu S, Chitsaz F, Geer LY, et al. CDD: NCBI's conserved domain database. Nucleic Acids Res. 2015;43(D1):D222–6.
39. Tian W, Chen C, Lei X, Zhao J, Liang J. CASTp 3.0: computed atlas of surface topography of proteins. Nucleic Acids Res. 2018;46(W1):W363–7.
40. Amano Y, Namatame I, Tateishi Y, Honboh K, Tanabe E, Niimi T, et al. Structural insights into the novel inhibition mechanism of *Trypanosoma cruzi* spermidine synthase. Acta Crystallogr D Biol Crystallogr. 2015;71:1879–89.
41. Volkamer A, Kuhn D, Rippmann F, Rarey M. DoGSiteScorer: a web server for automatic binding site prediction, analysis and druggability assessment. Bioinformatics. 2012;28(15):2074–5.
42. Jendele L, Krivak R, Skoda P, Novotny M, Hoksza D. PrankWeb: a web server for ligand binding site prediction and visualization. Nucleic Acids Res. 2019;47(W1):W345–9.
43. Sarma M, Borkotoky S, Dubey VK. Structure-based drug designing against *Leishmania donovani* using docking and molecular dynamics simulation studies: exploring glutathione synthetase as a drug target. J Biomol Struct Dyn. 2024;42(14):7628–36.
44. Vidhya VM, Dubey VK, Ponnuraj K. Identification of two natural compound inhibitors of *Leishmania donovani* spermidine synthase (SpdS) through molecular docking and dynamic studies. J Biomol Struct Dyn. 2018;36(10):2678–93.
45. Khare P, Gupta AK, Gajula PK, Sunkari KY, Jaiswal AK, Das S, et al. Identification of novel S-adenosyl-L-homocysteine hydrolase inhibitors through homology-model-based virtual screening, synthesis, and biological evaluation. J Chem Inf Model. 2012;52(3):777–91.
46. Sakyi PO, Broni E, Amewu RK, Miller WA III, Wilson MD, Kwofie SK. Homology modeling, de novo design of ligands, and molecular docking identify potential inhibitors of *Leishmania donovani* 24-sterol methyltransferase. Front Cell Infect Microbiol. 2022;12:859981.
47. Sheikh SY, Ansari WA, Hassan F, Faruqui T, Khan MF, Akhter Y, et al. Drug repositioning to discover novel ornithine decarboxylase inhibitors against visceral leishmaniasis. J Mol Recognit. 2023;36(7):e3021.
48. Kar RK, Ansari MY, Suryadevara P, Sahoo BR, Sahoo GC, Dikhit MR, et al. Computational elucidation of structural basis for ligand binding with *Leishmania donovani* adenosine kinase. Biomed Res Int. 2013;2013:609289.
49. Sakyi PO, Kwofie SK, Tuekpe JK, Gwira TM, Broni E, Miller WA III, et al. Inhibiting *Leishmania donovani* sterol methyltransferase to identify lead compounds using molecular modelling. Pharmaceuticals (Basel). 2023;16(3):330.
50. Vadloori B, Sharath AK, Prabhu NP, Maurya R. Homology modelling, molecular docking, and molecular dynamics simulations reveal the inhi-

bition of *Leishmania donovani* dihydrofolate reductase-thymidylate synthase enzyme by Withaferin-A. BMC Res Notes. 2018;11:246.
51. Viana JO, Weber KC, da Cruz LEG, Santos RO, Rocha GB, Jordão AK, et al. In silico structural insights and potential inhibitor identification based on the benzothiazole core for targeting *L. major* pteridine reductase 1. ACS Omega. 2025;10(1):306–17.
52. Rajasekaran R, Chen YPP. Probing the structure of *L. major* DHFR TS and structure based virtual screening of peptide library for the identification of anti-leishmanial leads. J Mol Model. 2012;18:4089–100.
53. Challapa-Mamani MR, Tomás-Alvarado E, Espinoza-Baigorria A, León-Figueroa DA, Sah R, Rodriguez-Morales AJ, et al. Molecular docking and molecular dynamics simulations in related to *Leishmania donovani*: an update and literature review. Trop Med Infect Dis. 2023;8(10):457.
54. Shakoori AM, Alhakami F, Sindi G, Alyahyawi AY, Alhazzaa RA. Molecular docking of daunorubicin and etoposide drugs against *Leishmania donovani*: a theoretical study. J Vector Borne Dis. 2024;61(3):369–75.
55. Singh S, Prajapati VK. Exploring actinomycetes natural products to identify potential multi-target inhibitors against *Leishmania donovani*. 3 Biotech. 2022;12(9):235.
56. Bora K, Sarma M, Kanaujia SP, Dubey VK. Dual-target drugs against *Leishmania donovani* for potential novel therapeutics. Sci Rep. 2023; 13:18363.
57. Wadanambi PM, Mannapperuma U. Computational study to discover potent phytochemical inhibitors against drug target, squalene synthase from *Leishmania donovani*. Heliyon. 2021;7(6):e07178.
58. Arthur MN, Hanson G, Broni E, Sakyi PO, Mensah-Brown H, Miller WA III, et al. Natural product identification and molecular docking studies of *L. major* pteridine reductase inhibitors. Pharmaceuticals (Basel). 2025;18(1):6.
59. Mansuri R, Diwan A, Mundotiya PK, Singh J. Structural analysis and in-silico inhibitor interaction studies of *Leishmania donovani* heat-shocked proteins 83 (HSP83). Int J Life Sci Pharma Res. 2023;13(Suppl 1):P8–18.
60. Arya PK, Barik K, Kumar A. Targeting spermidine synthase in *Leishmania donovani*: molecular docking and molecular dynamics simulation-based evaluation of Indian medicinal plant phytochemicals. In Silico Pharmacol. 2026;14(1):12.